NJC

PAPER

Cite this: *New J. Chem.*, 2023, **47**, 20557

Photoinduced hydrogen-bonded self-assembly of cation-capped complexes and novel photoswitchable supramolecular devices based on (aza)-18-crown-6-containing styryl dyes bearing a long *N*-ammonioalkyl substituent†

Sergey P. Gromov,*[ab] Timofey P. Martyanov,[ac] Artem I. Vedernikov,[a] Svetlana N. Dmitrieva,[a] Dmitry V. Kondratuk,[a] Artem P. Vorozhtsov[ac] and Evgeny N. Ushakov*[ac]

Received 21st June 2023,
Accepted 14th October 2023

DOI: 10.1039/d3nj02877a

rsc.li/njc

E-Isomers of styryl dyes containing a benzo-18-crown-6 ether or *N*-methylbenzoaza-18-crown-6 ether moiety and a benzothiazolium residue with an ammoniohexyl, ammoniopentyl, or ammonio-methylbenzyl *N*-substituent were synthesized. According to spectrophotometry and NMR spectroscopy data, dyes of this type are capable of self-assembly in MeCN to form dimeric complexes, which have a pseudocyclic structure owing to double intermolecular ammonium cation–crown ether interactions *via* hydrogen bonds; the dimerization equilibrium constants were measured. It was shown that photoinduced *Z*-isomers of the dyes are capable of intramolecular complex formation between the ammonium cation and the crown ether moiety; therefore, upon $E \rightarrow Z$ photoisomerization, the dimer–monomer equilibrium shifts towards the pseudocyclic monomer. Data on the relative stability of the intramolecular cation-capped complexes formed by *Z*-isomers were obtained. It was shown that the equilibrium constants for the Ba^{2+} complexation with *E*-isomers of the dyes are almost three orders of magnitude higher than those for that with *Z*-isomers, which may imply the applicability of these dyes as photoswitchable supramolecular devices.

1. Introduction

A molecular device (MD) is a molecular system consisting of two or more structurally organized components that accomplish a common specific function.[1–3] Each component performs only its own particular function; however, cooperation of the components gives rise to a more intricate behavior. At the cellular level, MDs are often encountered in nature where they are essential for the existence of life.[4] While designing MDs, scientists borrow some approaches from living organisms, for example, light-harvesting antennae (antenna effect) and others.[1–3] In science and engineering, MDs are used in molecular electronics,[5–7] drug delivery systems,[8,9] theranostics,[10,11] catalysis,[12] and a wide variety of sensors.[13,14] In some cases, non-covalent interactions are employed to combine structural moieties of MDs; hence, they can be designated as supramolecular devices. Supramolecular self-assembly makes it possible to stabilize the intermediates and states that possess practically useful properties, but are unstable under ambient conditions.[15–17] Light is the most convenient way to control supramolecular devices, because the energy and intensity of light can be varied over a wide range. Also, methods of organic synthesis enable fine tuning of the chromophore group in molecular systems. Crown ether-containing unsaturated molecules are highly promising building blocks,[18–21] as they are able to form host–guest complexes between the macrocyclic moiety and the metal or ammonium ions and also exhibit photochemical activity because of the presence of the ethylene moiety in the chromophore.

Previously, we showed that the crown ether-containing styryl dye (*E*)-**1a** (Chart 1) bearing a long-chain *N*-substituent with a terminal ammonium group forms an intramolecular pseudocyclic

[a] *Photochemistry Center of RAS, FSRC "Crystallography and Photonics", Russian Academy of Sciences, Novatorov str. 7A-1, Moscow 119421, Russian Federation. E-mail: spgromov@mail.ru*

[b] *Department of Chemistry, Lomonosov Moscow State University, Leninskie Gory 1-3, Moscow 119991, Russian Federation*

[c] *Federal Research Center of Problems of Chemical Physics and Medicinal Chemistry, Russian Academy of Sciences, Chernogolovka, Moscow Region 142432, Russian Federation. E-mail: e.n.ushakov@gmail.com*

† Electronic supplementary information (ESI) available: Experimental details and the NMR spectra of novel compounds. See DOI: https://doi.org/10.1039/d3nj02877a

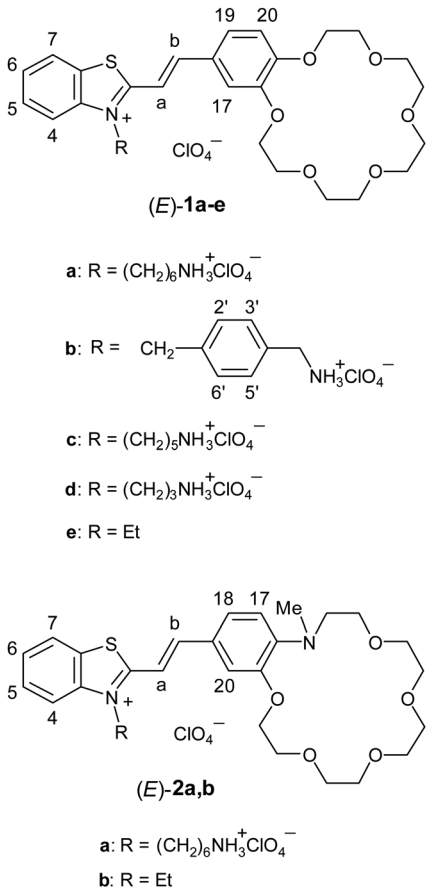

Chart 1 Crown ether styryl dyes (*E*)-**1** and (*E*)-**2**.

complex (cation-capped complex) as a result of $E \rightarrow Z$ photoisomerization.[22] In this complex, the ammonium group is coordinated to the crown ether oxygen atoms. We assumed that this would result in a lower efficiency of complex formation with metal ions for the *Z*-isomer of the dye compared with the *E*-isomer, due to competition for the crown ether cavity. Hence, the complexing capabilities of the two photoisomers would considerably differ. Thus, these compounds can be assigned to the class of photoswitchable supramolecular compounds called photoswitchable ionophores.[23–32]

In this study, we developed the synthesis and investigated the structure and photochemical and complexing properties of (aza)-18-crown-6 ether styryl dyes derived from 2-methylbenzothiazole (*E*)-**1a–c** and (*E*)-**2a** (Chart 1), which have a long-chain substituent with a terminal ammonium group at the N atom of the heterocyclic residue. Dyes (*E*)-**1d, e** and (*E*)-**2b**, which do not contain an ammonium group or have a relatively short ammonioalkyl *N*-substituent (Chart 1), were used as model compounds. An important feature of this study is that we used *N*-methylbenzoaza-18-crown-6 ether derivatives, which combine the benefits of both benzo-18-crown-6 ethers (high stability constants of complexes with metal or primary ammonium ions) and phenylaza-18-crown-6 ethers (large cation-induced spectral changes).[33]

2. Results and discussion

2.1 Synthesis of styryl dyes

Crown ether styryl dyes (*E*)-**1b, c** and (*E*)-**2a** (Chart 1) were synthesized using heterocyclic salts **3a–c** with ammonioalkyl and ammoniomethylbenzyl *N*-substituents (Scheme 1). The synthesis of compound **3a**[22] and dyes (*E*)-**1a**,[22] **d**,[34] **e**[22] and (*E*)-**2b**[35] was reported in our previous publications. Salts **3b, c** were obtained by quaternization of 2-methylbenzothiazole with 4-(bromomethyl)benzylammonium bromide[36] and 5-bromopentylammonium bromide,[37] respectively, followed by treatment with concentrated perchloric acid (Scheme 1).

Heterocyclic salts **3** were condensed with formyl benzo-18-crown-6 ether[38] and *N*-methylbenzoaza-18-crown-6 ether[39,40] derivatives in ethanol (for (*E*)-**1b, c**) or in ethanol containing some pyridine (for (*E*)-**2a**). This gave crown ether styryl dyes (*E*)-**1b, c** and (*E*)-**2a** in 50–65% yields (Scheme 2).

The structures of all the obtained compounds were determined using ^{1}H and ^{13}C NMR spectroscopy (see Fig. S1–S14 in the ESI†) and UV-vis spectrometry and confirmed using elemental analysis data. Styryl dyes (*E*)-**1b, c** and (*E*)-**2a** have the *E*-configuration of the ethylene bond, as inferred from the spin–spin coupling constants $^3J_{HC=CH}$ = 15.5–15.7 Hz.

2.2 ^{1}H NMR study

Previously, it was found using ^{1}H NMR spectroscopy that dyes (*E*)-**1a** and (*E*)-**1d** in MeCN-d$_3$ form *anti*-head-to-tail pseudocyclic dimers as a result of spontaneous self-assembly *via* hydrogen bonding between the terminal ammonium group of one dye molecule and the crown ether moiety of the other molecule (Scheme 3).[22,34]

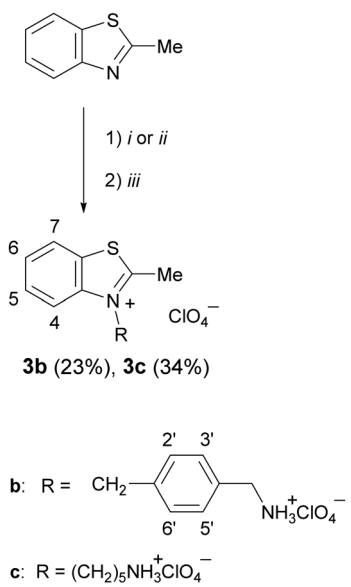

Scheme 1 Synthesis of compounds **3b, c**. *Reagents and conditions*: (*i*) 4-(bromomethyl)benzylammonium bromide, 100 °C; (*ii*) 5-bromopentylammonium bromide, 160 °C; (*iii*) $HClO_4$ (70%, aq.), MeOH (see the ESI,† Chapter SI).

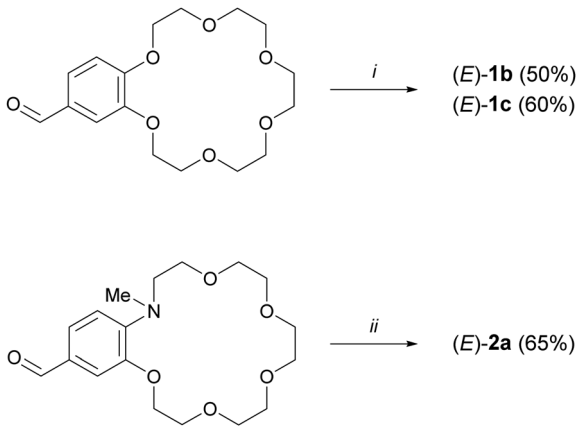

Scheme 2 Synthesis of dyes (*E*)-**1b, c** and (*E*)-**2a**. *Reagents and conditions*: (*i*) compound **3b** or **3c**, abs. EtOH, 80 °C; (*ii*) 3-(6-ammoniohexyl)-2-methyl-1,3-benzothiazol-3-ium diperchlorate (**3a**), pyridine, abs. EtOH, 80 °C (see the ESI,† Chapter SI).

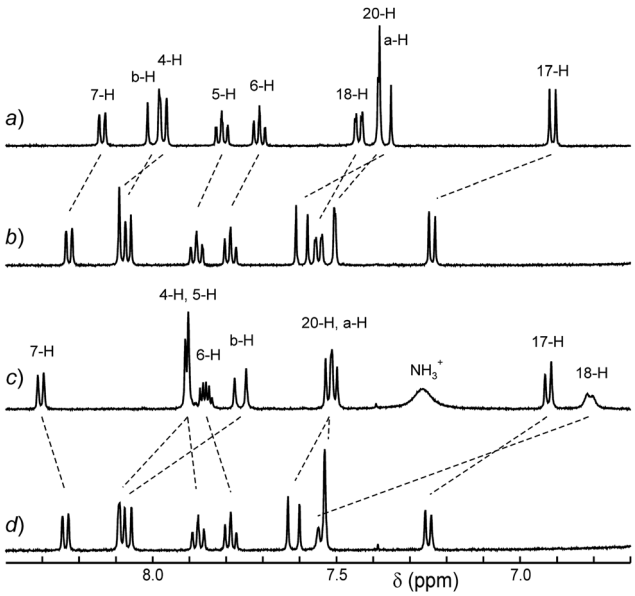

Fig. 1 ^{1}H NMR spectra (aromatic proton region) of dye (*E*)-**2b** (a), a mixture of (*E*)-**2b** and $EtNH_3ClO_4$ (1 : 3) (b), dye (*E*)-**2a** (c), and a mixture of (*E*)-**2a** and $EtNH_3ClO_4$ (1 : 49) (d) (C_{2b} = 5 × 10^{-3} M, C_{2a} = 3 × 10^{-3} M) in MeCN-d_3, 25 °C.

The structure of dimeric complex [(*E*)-**1a**]$_2$ in the crystal was proved using X-ray diffraction analysis.[41] The photoirradiation of dye (*E*)-**1a** in MeCN-d_3 gave rise to signals of the *Z*-isomer in the ^{1}H NMR spectra.[22] The spectral features of (*Z*)-**1a** attest to the formation of an intramolecular complex between the ammonium group and the crown ether moiety (Scheme 3).

The dimerization of the other ammonium dyes was confirmed by recording their ^{1}H NMR spectra in MeCN-d_3 and, for comparison, analogous spectra of model dyes (*E*)-**1e** and (*E*)-**2b** in the absence and in the presence of excess $EtNH_3ClO_4$. As an example, Fig. 1 shows a comparison of the aromatic proton regions in the spectra of free dyes (*E*)-**2a, b** and these dyes in the presence of excess $EtNH_3^+$ ions.

The addition of excess $EtNH_3ClO_4$ to a solution of (*E*)-**2b** induces downfield shifts of most dye protons by up to 0.33 ppm (Fig. 1a, b and Fig. S15a, b in the ESI†). This is evidently caused by the electron-withdrawing effect of the ethylammonium cation complexed with the azacrown ether moiety. Conversely, the proton signals of the CH_2NMe group shift upfield (by up to −0.32 ppm). This is caused by the conformational changes of *N*-methylbenzoazacrown ethers induced by binding to singly charged cations, particularly, CH_2N and MeN groups deviate from the deshielding plane of the benzene ring.[42] The spectra of dyes (*E*)-**2a, b** in the presence of excess $EtNH_3ClO_4$ are virtually identical regarding the position of signals of the same type (*cf.* Fig. 1b and d and Fig. S15b and d (ESI†)); this confirms that their complexes with the ethylammonium ions have the same structure. Meanwhile, the spectra of free dyes (*E*)-**2a** and (*E*)-**2b** markedly differ (*cf.* Fig. 1a, c and Fig. S15a, c, ESI†). In the aromatic proton region, the 4-H, b-H, and 18-H proton signals of dye (*E*)-**2a** considerably shift upfield (by up to −0.63 ppm) in comparison with the same proton signals of (*E*)-**2b**. This may be attributable to shielding of these protons in the *anti*-head-to-tail dimer [(*E*)-**2a**]$_2$ by the conjugated moiety of the neighboring molecule. The relatively small downfield shifts of other aromatic proton signals are obviously related to the electron-withdrawing effect of the ammonium group complexed with the azacrown ether moiety in dimer [(*E*)-**2a**]$_2$. In [(*E*)-**2a**]$_2$, the proton signals of the ammoniohexyl spacer are strongly shielded with respect to those for a mixture of (*E*)-**2a** with excess $EtNH_3^+$ ions (Fig. S15c and d, ESI†). This implies

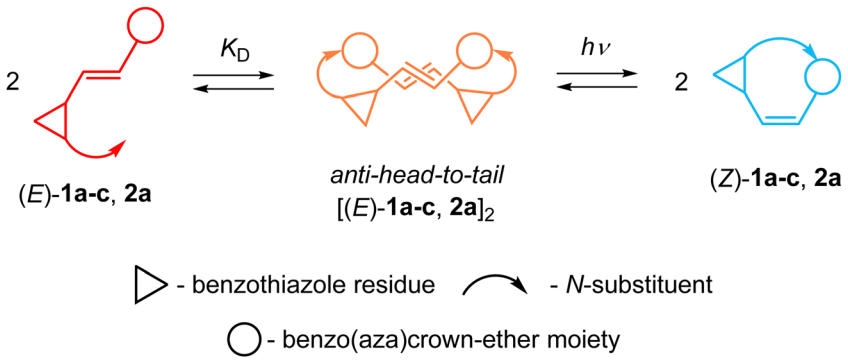

Scheme 3 Dimerization of dyes (*E*)-**1a–c** and (*E*)-**2a**, and photochemical conversion to monomers (*Z*)-**1a–c** and (*Z*)-**2a** as intramolecular complexes.

that these protons fall into the shielding region of the second dye molecule in the dimer. Similar spectroscopic characteristics were found previously for dyes (*E*)-**1a, d**.[22,34]

No intermolecular cross-peaks are present in the NOESY spectrum of (*E*)-**2a** (Fig. S16, ESI†). Apparently, distances between protons of neighboring molecules in the dimer complex [(*E*)-**2a**]$_2$ are longer than 3.5–4 Å, like in the crystalline complex [(*E*)-**1a**]$_2$ studied previously.[41]

Similar characteristics were found for new dyes (*E*)-**1b, c** when their spectral properties were compared with those of the model dye (*E*)-**1e** and those in the presence of excess $EtNH_3ClO_4$ (Fig. S17–S20, ESI†). Only unusually great shifts of some proton signals in the aromatic region are noteworthy in the case of (*E*)-**1b**. Apparently, these protons experience significant anisotropic effects from the ammoniomethylbenzyl group of the neighboring molecule, which is located closely in dimer [(*E*)-**1b**]$_2$.

Thus, we confirmed the pseudocyclic structure of the dimer complexes of styryl dyes (*E*)-**1b, c** and (*E*)-**2a** formed *via* hydrogen bonding between the ammonium group of one dye molecule and the (aza)crown ether moiety of the other molecule. It is clear that with this dimer structure, the conjugated moieties of the two dye molecules are located one above the other in the *anti*-head-to-tail fashion (Scheme 3).

The dimerization equilibrium constants K_D for ammonium dyes (*E*)-**1a–d** and (*E*)-**2a** and the stability constants K_S for the complexes of model dyes (*E*)-**1e** and (*E*)-**2b** with $EtNH_3^+$ ions measured by ^{1}H NMR titration with $EtNH_3ClO_4$ are presented in Table S1 (ESI†). Since the calculations were done with some assumptions (see the ESI†) and since it is impossible to maintain a constant ionic strength of the solution during ^{1}H NMR titration, $\log K_D$ values that we found were effective values corresponding to a simplified model of dimerization equilibrium with no allowance for dimer association with the anion (equilibrium (1) and (2)):

$$(E)\text{-}\mathbf{L} + EtNH_3^+ \overset{K_S}{\rightleftharpoons} (E)\text{-}\mathbf{L}\cdot EtNH_3^+, \quad (1)$$

$$(E)\text{-}\mathbf{L} + (E)\text{-}\mathbf{L} \overset{K_D}{\rightleftharpoons} [(E)\text{-}\mathbf{L}]_2, \quad (2)$$

where (*E*)-**L** is the *trans*-isomer of the dye (dication), (*E*)-**L**·$EtNH_3^+$ is the complex of the dye and ethylammonium ion, K_S is the stability constant of (*E*)-**L**·$EtNH_3^+$, [(*E*)-**L**]$_2$ is the dye dimer (tetracation), and K_D is the stability constant of dimer [(*E*)-**L**]$_2$.

The $\log K_D^{eff}$ values for the ammonioalkyl derivatives of dyes (*E*)-**1a, c, d** varied over a relatively narrow range of 5.9–6.3 [M^{-1}]. This indicates a rather high flexibility of the ammonioalkyl spacers and a weak stacking interaction of the conjugated moieties in the *anti*-head-to-tail dimer complexes. Dye (*E*)-**1b**, which had a conformationally more rigid ammoniomethylbenzyl spacer, formed somewhat less stable dimer complexes. Finally, on going from (*E*)-**1a** to (*E*)-**2a**, the dimerization constant considerably decreased ($\log K_D^{eff}$ = 4.3 [M^{-1}]). Apparently, in 2-benzothiazole styryl dyes, the *N*-methylbenzoaza-18-crown-6 ether moiety bound the primary ammonium ions more weakly compared to related dyes containing a benzo-18-crown-6 ether moiety. This conclusion supports the results of comparison of the stability constants K_S^{eff} for the complexes formed by model dyes (*E*)-**1e** and (*E*)-**2b** with $EtNH_3^+$. Note that at the qualitative level, these results are in line with the corresponding data obtained using spectrophotometry (Table 1).

Table 1 Results of a spectrophotometric study of self-complexation of (*E*)-**1a–c** and (*E*)-**2a** and LWAB characteristics for the *E*-isomers of model dyes **1e** and **2b** in MeCN[a]

				λ_{max}/nm		$\varepsilon_{max} \times 10^{-4}$/ M^{-1} cm^{-1}		
Dye	$\log K_D$	$\log K_A$	d_L/Å	Monomer	Dimer	Monomer	Dimer	$\log K_D^{eff}$
(*E*)-**1a**	4.06	3.85	12.4	431.5	411	3.57	6.70	5.70
(*E*)-**1b**	4.94	3.65	10.7	439	416	3.60	6.85	6.35
(*E*)-**1c**	4.32	3.99	10.7	433.5	411	3.57	6.73	6.05
(*E*)-**1e**				431		3.90		
(*E*)-**2a**	3.49	3.87	11.8	523	432	4.21	5.94	5.15
(*E*)-**2b**				526		4.30		

[a] d_L is the conventional diameter of the dye dication; λ_{max} is the position of the LWAB peak; ε_{max} is the corresponding molar absorption coefficient; and K_D^{eff} is the effective (observed) dimerization constant of the dye in the presence of a large excess (0.01 M) of the supporting electrolyte (Bu_4NClO_4).

2.3 UV-vis spectroscopy study

Solutions of (*E*)-**1a–c** and (*E*)-**2a** in MeCN have a deep and intense color at 380 and 560 nm, respectively, which is attributable to the ability of the lone pair of electrons of oxygen or nitrogen atoms located in the *para*-position to the C=C double bond in the crown ether moiety to be conjugated with the benzothiazole residue. Dye (*E*)-**2a**, in which the macrocycle nitrogen atom is conjugated with the chromophore group, absorbs at a longer wavelength than (*E*)-**1a–c**. This is due to more pronounced electron-donating properties of nitrogen. The absorption spectra of the dyes change considerably upon an increase in the dye concentration and/or addition of the tetrabutylammonium perchlorate (Bu_4NClO_4), acting as a supporting electrolyte (Fig. 2 for (*E*)-**2a**). The spectral changes attest to the formation of pseudocyclic dimer complexes (Scheme 3) *via* double intermolecular interactions between the ammonium group of one dye molecule and the crown ether moiety of the other molecule.

The long-wavelength absorption band (LWAB) in the spectra of dyes (*E*)-**1a–c** and (*E*)-**2a** is attributed to the electron transition accompanied by intramolecular charge transfer from the electron-donating benzocrown ether moiety to the electron-withdrawing benzothiazolium residue. After dimerization, the energy of this electron transition increases, since the hydrogen bonding between the ammonium cation and the crown ether moiety leads to a decrease in the electron-donating properties of the benzocrown ether moiety. This brings about blue shifts in the absorption spectrum. LWAB characteristics of the dimer complex can also be somewhat influenced by the stacking interaction between the two styryl chromophores. Usually, stacking interactions between the dye molecules in the dimer induce exciton splitting[43] of LWAB into two components, the more intense of which is blue-shifted and the less intense is red-shifted relative to the monomer band. Rather often, these

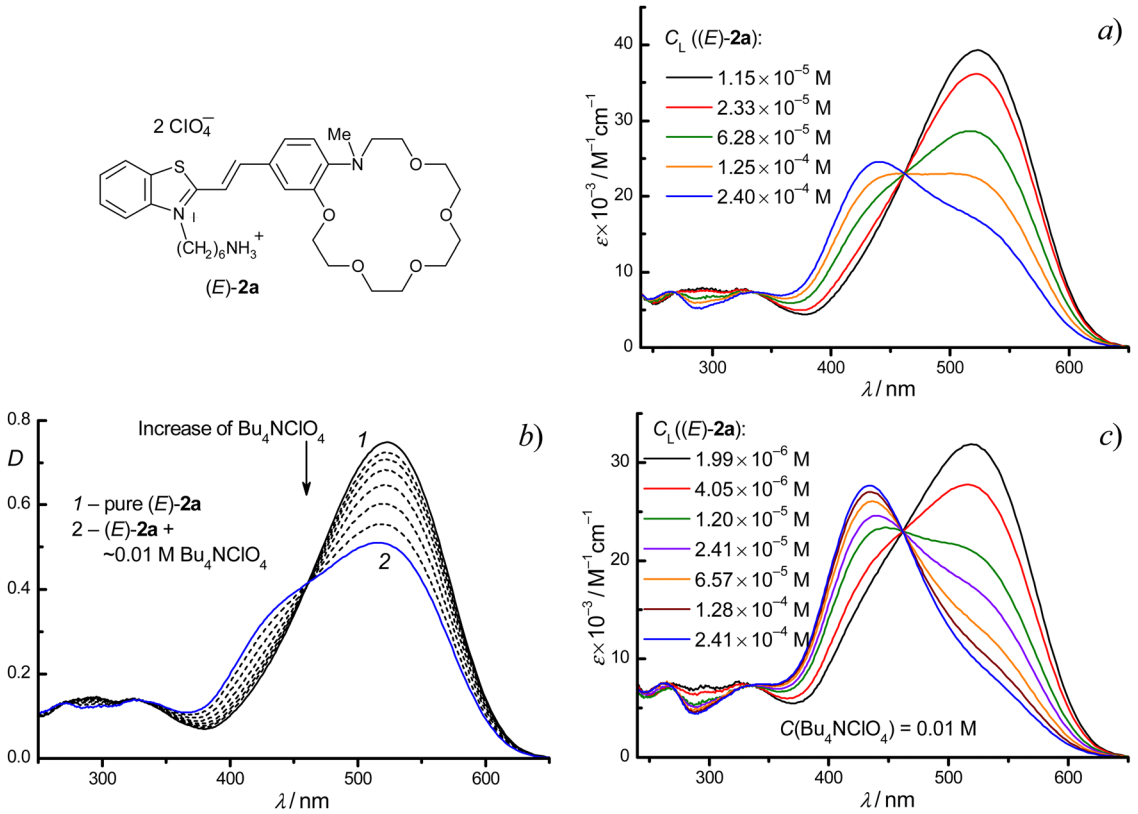

Fig. 2 (a) Absorption spectra of (*E*)-**2a** in MeCN measured at various dye concentrations (C_L) in quartz cells with different path lengths. (b) Absorption spectra of (*E*)-**2a** (C_L = 3.84 × 10^{-6} M, 4.75 cm cell) in MeCN measured at various concentrations (*SE*) of Bu_4NClO_4: *SE* = 0 (1), 1.83 × 10^{-4}, 3.66 × 10^{-4}, 7.38 × 10^{-4}, 1.48 × 10^{-3}, 2.96 × 10^{-3}, 5.86 × 10^{-3}, and 1.14 × 10^{-2} (2) M. (c) Absorption spectra of (*E*)-**2a** in MeCN measured at various dye concentrations in cells with different path lengths in the presence of a large excess of Bu_4NClO_4 (0.01 M).

two bands are unresolved, with the red-shifted band being detected only by LWAB broadening and by the presence of the long-wavelength shoulder.

Quantitative data on the dimerization of (*E*)-**2a** were obtained by analyzing the results of three experiments (Fig. 2): (a) absorption spectra of (*E*)-**2a** measured at various dye concentrations (in cells with different path lengths); (b) absorption spectra of the (*E*)-**2a**–Bu_4NClO_4 system measured at a constant dye concentration and various Bu_4NClO_4 concentrations; (c) absorption spectra of the (*E*)-**2a**–Bu_4NClO_4 system measured at various dye concentrations (in cells with different path lengths) and a constant Bu_4NClO_4 concentration (0.01 M). Only two experiments (a and b) were carried out for (*E*)-**1a–c**, as the variation of the spectra in experiment (c) was insignificant. The concentration changes in the absorption spectra of (*E*)-**1a–c** were qualitatively similar to those observed for (*E*)-**2a**.

The attempts to describe the concentration dependences of the absorption spectra of (*E*)-**1a–c** and (*E*)-**2a** in terms of a simple dimerization model including only one equilibrium (2) failed. Using a heuristic approach, we found that these dependences can be described in terms of the reaction model that includes two equilibriums (2) and (3).

$$[(E)\text{-}\mathbf{L}]_2 + \mathrm{A} \overset{K_A}{\rightleftharpoons} (E)\text{-}\mathbf{L}\cdot\mathrm{A}\cdot(E)\text{-}\mathbf{L}, \qquad (3)$$

where A is the anion (ClO_4^-), (*E*)-**L**·A·(*E*)-**L** is the triply charged associate of the dimer with the anion, and K_A is the stability constant of associate (*E*)-**L**·A·(*E*)-**L**. The absorption spectra of the monomers and dimers of (*E*)-**1a–c** and (*E*)-**2a** and the equilibrium constants K_D and K_A were determined using parameterized matrix modeling (PMM)[44] of the spectral data (Fig. 2). The activity coefficients of ions, calculated using the second approximation of the Debye–Hückel formula, were taken into account in the law of mass action and mass balance equations (see the ESI,† Chapter SVII).

The concentration-dependent absorption spectra of dyes (*E*)-**1a–c** and (*E*)-**2a** in their most variable range (350–520 nm for (*E*)-**1a–c** and 350–640 nm for (*E*)-**2a**) were well reproduced by the PMM method on the basis of equilibria (2) and (3) (the standard deviation σ_D was below 0.0014 in all cases). This is illustrated in Fig. 3, which shows the absorption spectra of (*E*)-**2a** from three experiments and the theoretical spectra derived from equilibria (2) and (3) by PMM with K_D = 3.1 × 10^3 M^{-1}, K_A = 7.4 × 10^3 M^{-1}, and the dye dication diameter d_L = 11.8 Å (σ_D = 0.0013).

Table 1 summarizes the results of the spectrophotometric study of the self-complexation of (*E*)-**1a–c** and (*E*)-**2a** in MeCN: $\log K_D$, $\log K_A$, and d_L values, LWAB characteristics of the monomers and dimers (λ_{max} and ε_{max}), and effective equilibrium constants of dimerization ($\log K_D^{eff}$) in the presence of a large excess (0.01 M) of the supporting electrolyte (Bu_4NClO_4).

In the series of dyes (*E*)-**1a–c**, the equilibrium constant K_D and the effective dimerization constant K_D^{eff} change insignificantly.

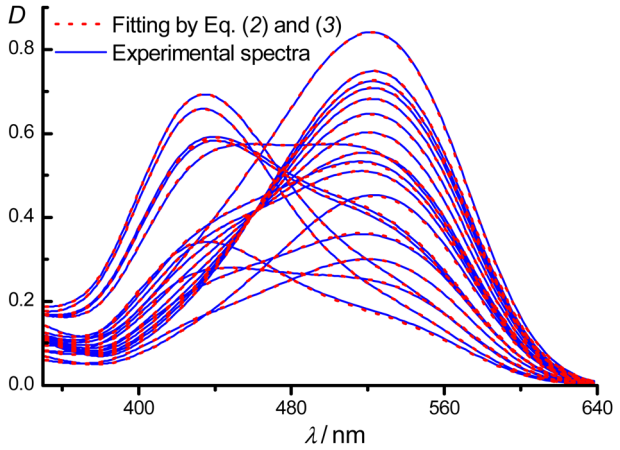

Fig. 3 Absorption spectra of dye (*E*)-**2a** from three different experiments described in the text (blue curves) and theoretical spectra (red points) obtained by PMM based on equilibria (2) and (3) with K_D = 3.1 × 10^3 M^{-1}, K_A = 7.4 × 10^3 M^{-1}, and d_L = 11.8 Å.

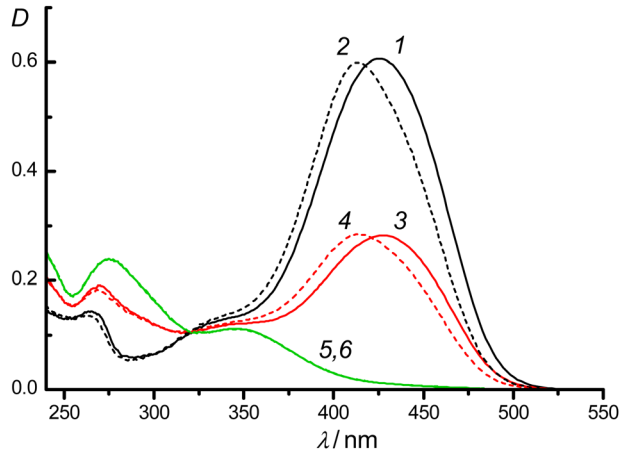

Fig. 4 Absorption spectra of dye **1a** in MeCN (C_L = 1.8 × 10^{-5} M, 1 cm cell): (*1*, *2*) (*E*)-**1a** in the absence and in the presence of Bu_4NClO_4 (*SE* = 0.01 M), respectively; (3–6) photostationary equilibria attained upon irradiation of solutions *1* and *2* at 365 (*3*, *4*) and 436 (*5*, *6*) nm.

Dye (*E*)-**2a** has a lower tendency to dimerization than (*E*)-**1a–c**, apparently, due to a lower ability of its azacrown ether moiety to coordinate the ammonium cation.

2.4 Photoisomerization of free dyes

Visible light irradiation of (*E*)-**1a–c** and (*E*)-**2a** in solutions induced pronounced changes in their absorption spectra typical of *E*→*Z* photoisomerization. In the case of dye **1a**, irradiation at λ = 436 nm results in almost complete disappearance of LWAB of the *E*-isomer (Fig. 4), while the spectrum of the formed *Z*-photoisomer does not depend on the degree of dimerization of the initial *E*-isomer (to shift the dimerization equilibrium of (*E*)-**1a** towards the dimer, Bu_4NClO_4 was added). Note also the abnormally large blue shift of LWAB of (*Z*)-**1a** relative to LWABs of the *E*-isomer monomer and dimer, $\Delta\lambda_{EZ}$ = 85.5 and 65 nm, respectively. For model dye **1e**, $\Delta\lambda_{EZ}$ is only 11 nm (Fig. S21, ESI†).

These facts can be interpreted under the assumption that the geometry of (*Z*)-**1a** allows the formation of an intramolecular coordination bond (ICB) between the ammonium group in the *N*-substituent and the crown ether moiety, *i.e.*, (*Z*)-**1a** in a dilute solution exists as a pseudocyclic intramolecular complex (PIC, or cation-capped complex, Scheme 3). Apparently, the PIC formation is accompanied by a pronounced increase in the torsion angles in the Het–C═C and Ar–C═C moieties, which leads to a strong disruption of the conjugation in the Het–C═C–Ar chain. As a result, the intramolecular charge-transfer electronic transition ($S_0 \rightarrow S_1$) becomes forbidden, and the $S_0 \rightarrow S_1$ band in the spectrum of (*Z*)-**1a** is unobservable. In other words, LWAB of (*Z*)-**1a** is, most likely, mainly related to the local electronic transitions in the benzothiazole residue. This conclusion can be drawn from comparison of the spectra of (*Z*)-**1e** and (*Z*)-**1a** (see Fig. S21, ESI† and 4, respectively). The spectrum of *Z*-isomeric model dye **1e** exhibits two broad bands at >300 nm: the $S_0 \rightarrow S_1$ band with λ_{max} = 411 nm corresponds to intramolecular charge-transfer electronic transition, while the $S_0 \rightarrow S_2$ band at λ_{max} = 308 nm is apparently related to a local electronic transition in the benzothiazolium residue. In the spectrum of (*Z*)-**1a**, the $S_0 \rightarrow S_1$ band has a very low intensity, while the $S_0 \rightarrow S_2$ band is red-shifted by 38 nm relative to this band in the spectrum of (*Z*)-**1e**.

Irradiation of (*E*)-**1b, c** at λ_{max} = 436 nm and (*E*)-**2a** at λ_{max} = 546 nm also led to the photostationary equilibria with a very high content of the *Z*-isomer (>90%), which indicated that the *Z*-isomers of these dyes, like (*Z*)-**1a**, exist as PICs.

The absorption spectra of pure *Z*-photoisomers of **1a–c** and **2a** and the ratios of the quantum yields of the forward and reverse photoisomerization, φ_{E-Z}(monomer)/φ_{Z-E} and φ_{E-Z}(dimer)/φ_{Z-E}, were calculated from the spectra of the photostationary states attained upon the irradiation of *E*-isomer solutions at various wavelengths. In each case, at least two experiments were carried out using solutions with the same total concentration of the dye, but different degrees of dimerization of the starting *E*-isomer (to shift the equilibrium towards the dimer, Bu_4NClO_4 was added). The calculations were based on the assumption that the φ_{E-Z}(monomer)/φ_{Z-E} and φ_{E-Z}(dimer)/φ_{Z-E} ratios do not depend on the irradiation wavelength. The known spectra of the monomers and dimers of (*E*)-**1a–c** and (*E*)-**2a** were used in the calculations. High calculation accuracy was attained by using the PMM procedure. These calculations resulted in the spectra of pure *Z*-isomers and the φ_{E-Z}(monomer)/φ_{Z-E} and φ_{E-Z}(dimer)/φ_{Z-E} values. The results were then used to determine the quantum yields φ_{E-Z}(monomer), φ_{E-Z}(dimer), and φ_{Z-E}.

The φ_{E-Z}(monomer), φ_{E-Z}(dimer), and φ_{Z-E} values for **1a–c** were derived from the kinetics of the absorption spectra observed under steady-state irradiation of the initial *E*-isomer in solution at λ = 365 nm. For dye **2a**, the φ_{E-Z}(monomer) and φ_{E-Z}(dimer) values proved to be much lower than φ_{Z-E}; in this case, φ_{E-Z}(monomer) and φ_{E-Z}(dimer) were found from the kinetics of consumption of the *E*-isomer under steady-state irradiation at λ = 546 nm where the (*Z*)-**2a** does not absorb. The kinetic data were processed taking into account the slow

dark $Z \rightarrow E$ isomerization. To measure φ_{Z-E}, first, a solution with a high (*Z*)-**2a** content (>90%) was obtained (by irradiation of a (*E*)-**2a** solution at λ = 546 nm). Then this solution was irradiated at λ = 365 nm, and the φ_{Z-E} value was determined from the observed accumulation kinetics of the *E*-isomer (when **2a** is irradiated at λ = 365 nm, the photostationary equilibrium is in fact completely shifted towards the *E*-isomer).

The key results of the photochemical investigation of dyes **1a–c** and **2a**, *i.e.*, the quantum yields φ_{E-Z}(monomer), φ_{E-Z}(dimer), and φ_{Z-E} and the LWAB characteristics of the *Z*-isomers are summarized in Table 2.

The absorption spectra of (*Z*)-**1a–c** and (*Z*)-**2a** (Fig. S22, ESI†) are similar, but they differ significantly from the spectrum of the *Z*-isomer of model dye **1e** (Fig. S21, ESI†), since (*Z*)-**1a–c** and (*Z*)-**2a**, unlike (*Z*)-**1e**, exist as PICs. The presence of ICB in the *Z*-isomers of **1a–c** and **2a** has almost no effect on the quantum yield of the $Z \rightarrow E$ photoisomerization. In all of the four cases, the φ_{Z-E} values are about 0.5, which is a typical value for isomerization reactions proceeding by a non-adiabatic mechanism through a twisted phantom state (the deviations of φ_{Z-E} from 0.5 do not exceed 20%, *i.e.*, they are within the error of measurements). The $E \rightarrow Z$ photoisomerization is also quite efficient for the monomers of crown ether dyes (*E*)-**1a–c**. In the case of dimers of (*E*)-**1a–c**, the quantum yields φ_{E-Z} are 30–40% lower than those for the monomers. This may be due to steric hindrance for the transition of the excited *E*-isomer existing as a part of the pseudocyclic dimer complex to the twisted phantom state. The benzene ring present in the *N*-substituent at the benzothiazole residue of **1b** has a noticeable effect on the efficiency of $E \rightarrow Z$ photoisomerization: the φ_{E-Z}(monomer) and φ_{E-Z}(dimer) values are approximately 30% lower for **1b** than for **1a** or **1c**.

The $E \rightarrow Z$ photoisomerization of azacrown-containing dye **2a** has a low efficiency: the φ_{E-Z}(monomer) and φ_{E-Z}(dimer) values are <0.01. It is noteworthy that the luminescence quantum yields for the monomer and dimer of (*E*)-**2a** are also very low (approximately 0.004 and 0.005, respectively). In addition, the blue shift of the dimer luminescence band relative to the monomer luminescence band (Fig. S23, ESI†) is very small ($\Delta\lambda^{fl}_{max}$ = 8 nm) in comparison with the LWAB shift ($\Delta\lambda^{abs}_{max}$ = 91 nm). These facts can be interpreted as follows:

(1) Probably, in the charge transfer excited state, (*E*)-**2a** (monomer) undergoes conformational changes associated with the rotation of dye moieties relative to single bonds, resulting in the formation of the so-called twisted state with a higher degree of charge separation (TICT state). Due to high electron-donating ability of the benzoazacrown ether moiety in **2a**, the transition to the non-radiative TICT state is markedly faster than the transition to the non-radiative phantom state (the result of C=C bond twisting), which leads to the $E \rightarrow Z$ isomerization.

(2) The excitation of molecule (*E*)-**2a** existing as a part of the dimer probably induces recoordination reaction, *i.e.*, the hydrogen bond between the nitrogen atom of the benzoazacrown ether moiety of this molecule and the ammonium group of the other molecule in the dimer is disrupted. As a result, the excited molecule may be deactivated *via* non-radiative TICT state.

The *Z*-isomer of dye **1d**, which has a relatively short ammoniopropyl *N*-substituent, cannot form ICB. This is evidenced by the fact that the absorption spectrum of the photostationary state reached upon irradiation of **1d** at λ = 436 nm closely resembles the corresponding spectrum measured for model dye **1e** (Fig. S24, ESI†).

Table 2 LWAB characteristics of the *Z*-isomers and quantum yields of the forward and reverse $E \rightarrow Z$ photoisomerization for dyes **1a–c**, **e** and **2a** in MeCN[a]

Dye	λ^{Z}_{max}/nm	$\varepsilon^{Z}_{max} \times 10^{-4}$/M^{-1} cm^{-1}	φ_{E-Z} Monomer	φ_{E-Z} Dimer	φ_{Z-E}
1a	346	6.1	0.40	0.26	0.52
1b	359	5.9	0.29	0.17	0.59
1c	347	6.2	0.40	0.28	0.54
1e	420	8.6	0.38	—	0.49
2a	354	7.4	0.0028	0.0068	0.43

[a] The quantum yields are measured to be within about ±20%.

2.5 Complexation of *E*-isomers with metal ions

The stability constants and the absorption spectra of the complexes of these dyes with sodium and alkaline earth metal perchlorates were determined by PMM using the spectrophotometric titration (SPT) data and the assumed reaction model (Scheme 4).

In the case of direct titration of model dyes (*E*)-**1e** and (*E*)-**2b**, we used only one equilibrium,

$$(E)\text{-}\mathbf{L} + \mathrm{M} \overset{K_E}{\rightleftharpoons} (E)\text{-}\mathbf{L}\cdot\mathrm{M}, \quad (4)$$

where M is the metal ion and K_E is the stability constant of (*E*)-**L**·M. The measured constants were effective values (K_E^{eff}), since the activity coefficients were not taken into account in the calculations. In the processing of direct SPT data for dyes **1a** and **2a**, containing a long *N*-ammoniohexyl substituent, the complexation model included, apart from equilibrium (4), also

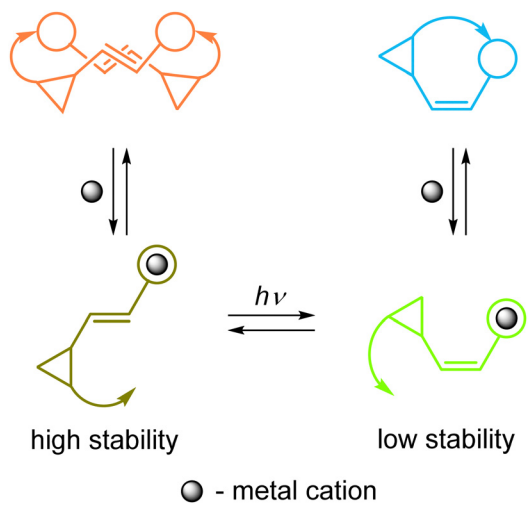

Scheme 4 Complexation of dimers [(*E*)-**1a–c**]$_2$ and [(*E*)-**2a**]$_2$, and of monomers (*Z*)-**1a–c** and (*Z*)-**2a**.

the dimerization eqn (2). In this case, the known absorption spectra of dye monomers and dimers and the known K_D^{eff} values were used in the calculations (Table 1). The stability constants of the complexes formed by (*E*)-**1a, b, e** with the Ba^{2+} ions were determined using the competitive SPT data against $NaClO_4$.

The addition of sodium, calcium, or barium perchlorate to solutions of model dyes (*E*)-**1e** and (*E*)-**2b** induced a blue shift of LWAB (Fig. S25–S29, ESI†). This effect is especially pronounced for azacrown ether derivative **2b** (up to 127 nm, Table 3). The absorption spectra of dyes (*E*)-**1a** and (*E*)-**2a** change in the presence of metal salts (Fig. 5). Apparently, due to complex formation between the metal cation and the monomer, the monomer–dimer equilibrium shifts towards the monomer.

The spectral characteristics and thermodynamic stability of complexes of (*E*)-**1a, b, e** and (*E*)-**2a, b** with metal cations are summarized in Table 3.

It can be seen (Table 3) that the stability of complexes of azacrown ethers (*E*)-**2a, b** is lower than the stability of complexes formed by crown ether analogues (*E*)-**1a, b, e**. A probable reason is the reduced electron-donating capacity of the azacrown nitrogen atom in (*E*)-**2a, b** because of high delocalization of its lone pair. Also in terms of the hard and soft (Lewis) acid and base principle, nitrogen is a softer base than oxygen and, hence, it interacts less efficiently with hard acids such as alkali and alkaline earth metal cations. The absolute values of the stability constants and their dependences on the metal cation nature for the complexes of dyes (*E*)-**1a, b, e** are typical of benzo-18-crown-6 ether derivatives.[45]

2.6 Complexation of *Z*-isomers with barium ions

In order to obtain comparative data on the thermodynamic stability of PICs for (*Z*)-**1a–c** and **2a**, we studied their complexation with Ba^{2+} ions at a constant ionic strength of 0.01 M (Scheme 4). Before SPT, a dye solution containing 0.01 M of the supporting electrolyte (Bu_4NClO_4) was irradiated at λ = 436 nm (for **1a–c**) until a photostationary state was reached. The content of the *Z*-isomer in this equilibrium state was >90% in all cases. Then the obtained solution was titrated with a $Ba(ClO_4)_2$ solution (Fig. 6) in such a way that the ionic strength of the dye solution did not change.

Table 3 Effective stability constants and LWAB characteristics of complexes of styryl dye *E*-isomers with metal cations[a]

Complex	λ_{max}/nm	$\Delta\lambda_{max}$/nm	$\varepsilon_{max} \times 10^{-4}$/M^{-1} cm^{-1}	$\log K_E^{eff}$
(*E*)-**1a**·Na^+	422	9.5	3.66	4.66
(*E*)-**1a**·Ca^{2+}	407	24.5	3.50	7.69
(*E*)-**1a**·Ba^{2+}	408	23.5	3.67	8.85
(*E*)-**1b**·Na^+	427	12	3.29	4.65
(*E*)-**1b**·Ba^{2+}	415	24	3.36	8.51
(*E*)-**1e**·Na^+	421	10	3.87	4.77
(*E*)-**1e**·Ba^{2+}	407	24	3.82	8.97
(*E*)-**2a**·Ca^{2+}	401	122	3.54	7.01
(*E*)-**2a**·Ba^{2+}	410	113	3.62	7.51
(*E*)-**2b**·Na^+	443	82	3.08	3.69
(*E*)-**2b**·Ca^{2+}	398	127	3.50	7.03
(*E*)-**2b**·Ba^{2+}	410	115	3.55	7.70

[a] λ_{max} is the long-wavelength absorption maximum, $\Delta\lambda_{max} = \lambda_{max}$ (monomeric dye) − λ_{max} (complex), and ε_{max} is the molar absorptivity coefficient at λ_{max}.

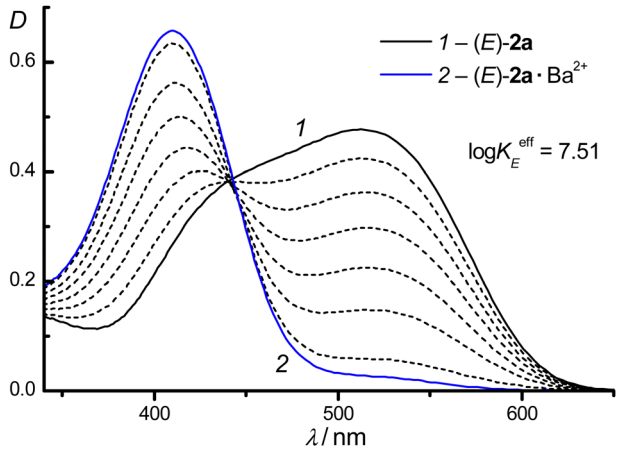

Fig. 5 Absorption spectra of the (*E*)-**2a**–$Ba(ClO_4)_2$ system in MeCN: 4.75 cm cell, constant ligand concentration (3.8×10^{-6} M), and variable $Ba(ClO_4)_2$ concentration (from 0 to 2.8×10^{-5} M); the ionic strength was maintained at 0.01 M by the supporting electrolyte (Bu_4NClO_4).

In the case of **2a**, the *E*–*Z* photostationary state with a high content of *Z*-isomer was obtained under irradiation at λ = 546 nm. The obtained spectrophotometric data were treated by the PMM method using equilibria (2), (4), and (5):

$$(Z)\text{-}\mathbf{L} + \mathrm{M} \overset{K_Z}{\rightleftharpoons} (Z)\text{-}\mathbf{L}\cdot\mathrm{M} \qquad (5)$$

where M is the metal ion (in our case, Ba^{2+}), K_Z is the stability constant of complex (*Z*)-**L**·M. The absorption spectra of the pure *Z*-isomers and monomers and dimers of (*E*)-**1a–c** and (*E*)-**2a** and also the known K_D^{eff} and K_E^{eff} values were used in the calculations. The application of the PMM procedure provided the K_Z^{eff} value and the absorption spectra of *Z*-isomer complexes with Ba^{2+}. The variation of K_E^{eff} in the 10^7–10^9 M^{-1} range had virtually no effect on the accuracy of approximation of the experimental spectra and on the main results.

The equilibrium constants for the complexation of Ba^{2+} with (*Z*)-**1a–c** and (*Z*)-**2a** are summarized in Table 4.

The fact that the complexation constant with Ba^{2+} is more than three orders of magnitude lower for (*Z*)-**1a** than for monomeric (*E*)-**1a** confirms the conclusion that (*Z*)-**1a** exists as PIC. As the ammoniohexyl chain length of **1a** decreases by one unit, that is, for dye **1c**, the K_Z^{eff} value increases by almost 1.5 orders of magnitude. This indicates that the ammoniopentyl chain length is critical for the formation of ICB in the *Z*-isomer of the dye, *i.e.*, on further shortening of this chain, the formation of ICB in the *Z*-isomer would, most likely, be impossible. Previously, a similar result was obtained using quantum chemical calculations of the formation energy of PIC for (*Z*)-**1a–d**.[41] Dye **1b** attracted attention due to its very low K_Z^{eff} value. This means that the conformationally rigid *N*-substituent in this dye is structurally pre-organized to form ICB in the *Z*-configuration of the styryl chromophore. As follows from the obtained stability constants of the *E*-isomers (Table 3), the K_E^{eff} value for complex (*E*)-**1b**·Ba^{2+} is much higher

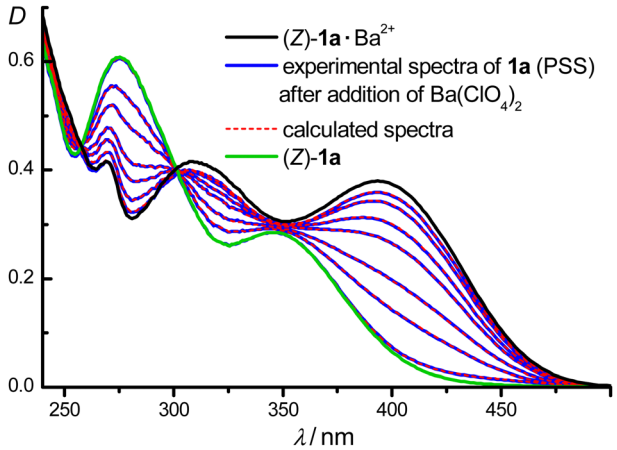

Fig. 6 Absorption spectra of dye **1a** in MeCN measured after the photostationary state (PSS) was established under irradiation at λ = 436 nm ((*Z*)-**1a** content >99%) and after addition of a few portions of a $Ba(ClO_4)_2$ solution (blue curves); 4.75 cm cell; initial dye concentration C_L = 9.8 × 10^{-6} M; concentration range of the metal salt of 0–8 × 10^{-5} M; and Bu_4NClO_4 as the supporting electrolyte (0.01 M). The red dashed curves are the model spectra obtained by the PMM method based on equilibria (2), (4), and (5). The black curve is the spectrum of (*Z*)-**1a**·Ba^{2+} obtained by PMM. The green curve is the spectrum of (*Z*)-**1a**.

Table 4 Effective stability constants of the complexes formed by (*Z*)-**1a–c** and (*Z*)-**2a** with Ba^{2+} in MeCN at a solution ionic strength of 0.01 M

Dye	(*Z*)-**1a**	(*Z*)-**1b**	(*Z*)-**1c**	(*Z*)-**2a**
$\log K_Z^{\mathrm{eff}}$	5.24	3.72	6.62	4.62

($\log K_E^{\mathrm{eff}}$ = 8.51) than the constant for the analogous complex of (*Z*)-**1b**. Thus, photoisomerization of dye **1b** changes the stability of the barium complex by almost five orders of magnitude.

3. Conclusions

We developed the synthesis of the *E*-isomers of styryl dyes containing a benzo-18-crown-6 ether (**1a–c**) or *N*-methylbenzoaza-18-crown-6 ether (**2a**) moiety and a benzothiazole residue with an ammoniohexyl (**1a**, **2a**), ammoniopentyl (**1c**), or ammoniomethylbenzyl (**1b**) *N*-substituent. It was shown that in MeCN, dyes (*E*)-**1a–c** and (*E*)-**2a** can self-assemble into dimeric complexes, which have a pseudocyclic structure owing to the double ammonium cation–crown ether intermolecular interaction through hydrogen bonding. The dimerization equilibrium constant changes insignificantly in the series (*E*)-**1a–c**. Compound (*E*)-**2a** has a lower tendency for dimerization, apparently, due to lower ability of its macroheterocyclic moiety to coordinate to the ammonium cation.

The monomers and dimers of (*E*)-**1a–c** and (*E*)-**2a** can undergo $E \rightarrow Z$ isomerization under visible light irradiation; the reverse $Z \rightarrow E$ isomerization can be induced thermally or by UV irradiation. It was shown that photoinduced *Z*-isomers of dyes **1a–c** and **2a** are capable of the intramolecular ammonium cation—crown ether complexation; therefore, after $E \rightarrow Z$ photoisomerization, the dimer–monomer equilibrium shifts towards the pseudocyclic monomer. The dependence of the thermodynamic stability of the intramolecular complex of the *Z*-isomer on the length and conformational rigidity of the substituent bearing the terminal ammonium group was determined. The supramolecular photoswitches of this structure may be of interest for the design of optical data recording systems.

It was ascertained that the equilibrium constants for the complex formation of Ba^{2+} with (*E*)-**1a–c** and (*E*)-**2a** are several orders of magnitude greater than those for that with the *Z*-isomers. This implies the possible applicability of these dyes as photoswitchable supramolecular devices such as photoswitchable ionophores. The greatest difference between the stability constants of the complexes of the *E*- and *Z*-isomers with Ba^{2+} is characteristic of dye **1b**, which has a conformationally rigid ammoniomethylbenzyl *N*-substituent, structurally pre-organized towards the formation of an intramolecular coordination bond in the *Z*-configuration of the styryl chromophore.

These results may also be useful for the development of artificial transmembrane ion channels that can be controlled by light and membranes with photocontrolled ion conductivity, and for photocontrolled extraction.

Conflicts of interest

There are no conflicts to declare.

Acknowledgements

This work was supported by the Russian Science Foundation (project no. 22-13-00064, except the spectrophotometric study of dye dimerization and NMR titrations). The measurement of the equilibrium constants of the dimerization reactions by spectrophotometry was done under financial support of the Ministry of Science and Higher Education of the Russian Federation (State Assignments no. AAAA-A19-119070790003-7). NMR titrations were carried out within the State assignment of FSRC "Crystallography and Photonics" of the RAS.

Notes and references

1 V. Balzani, A. Credi and M. Venturi, Molecular devices and machines, *Nano Today*, 2007, **2**(2), 18–25, DOI: 10.1016/S1748-0132(07)70055-5.
2 V. Balzani, A. Credi and M. Venturi, *Molecular Devices and Machines: Concepts and Perspectives for the Nanoworld*, Wiley-VCH Verlag GmbH & Co. KGaA, Weinheim, 2nd edn, 2008.
3 P. Ceroni, A. Credi and M. Venturi, Light to investigate (read) and operate (write) molecular devices and machines, *Chem. Soc. Rev.*, 2014, **43**, 4068–4083, DOI: 10.1039/c3cs60400d.
4 D. S. Goodsell, *Bionanotechnology – Lessons from Nature*, Wiley-Liss, Hoboken, 2004.

5 M. J. Latter and S. J. Langford, Porphyrinic Molecular Devices: Towards Nanoscaled Processes, *Int. J. Mol. Sci.*, 2010, **11**, 1878–1887, DOI: 10.3390/ijms11041878.

6 N. Xin, J. Guan, C. Zhou, X. Chen, C. Gu, Y. Li, M. A. Ratner, A. Nitzan, J. F. Stoddart and X. Guo, Concepts in the design and engineering of single-molecule electronic devices, *Nat. Rev. Phys.*, 2019, **1**, 211–230, DOI: 10.1038/s42254-019-0022-x.

7 J.-P. Collin, F. Durola, J. Luxa and J.-P. Sauvage, A copper-based shuttling [2]rotaxane with two bidentate chelates in the axis: steric control of the motion, *New J. Chem.*, 2010, **34**, 34–43, DOI: 10.1039/B9NJ00296K.

8 A. Rösler, G. W. M. Vandermeulen and H.-A. Klok, Advanced drug delivery devices *via* self-assembly of amphiphilic block copolymers, *Adv. Drug Delivery Rev.*, 2012, **64**, 270–279, DOI: 10.1016/j.addr.2012.09.026.

9 V. Linko, A. Ora and M. A. Kostiainen, DNA Nanostructures as Smart Drug-Delivery Vehicles and Molecular Devices, *Trends Biotechnol.*, 2015, **33**(10), 586–594, DOI: 10.1016/j.tibtech.2015.08.001.

10 H. Cabral, N. Nishiyama and K. Kataoka, Supramolecular Nanodevices: From Design Validation to Theranostic Nanomedicine, *Acc. Chem. Res.*, 2011, **44**(10), 999–1008, DOI: 10.1021/ar200094a.

11 I. L. Sokolov, V. R. Cherkasov, A. A. Tregubov, S. R. Buiucli and M. P. Nikitin, Smart materials on the way to theranostic nanorobots: Molecular machines and nanomotors, advanced biosensors, and intelligent vehicles for drug delivery, *Biochim. Biophys. Acta, Gen. Subj.*, 2017, **1861**(6), 1530–1544, DOI: 10.1016/j.bbagen.2017.01.027.

12 L. van Dijk, M. J. Tilby, R. Szpera, O. A. Smith, H. A. P. Bunce and S. P. Fletcher, Molecular machines for catalysis, *Nat. Rev. Chem.*, 2018, **2**, 0117, DOI: 10.1038/s41570-018-0117.

13 C. Guo, A. C. Sedgwick, T. Hirao and J. L. Sessler, Supramolecular fluorescent sensors: An historical overview and update, *Coord. Chem. Rev.*, 2021, **427**, 213560, DOI: 10.1016/j.ccr.2020.213560.

14 I. S. Antipin, M. V. Alfimov, V. V. Arslanov, V. A. Burilov, S. Z. Vatsadze, Y. Z. Voloshin, K. P. Volcho, V. V. Gorbatchuk, Y. G. Gorbunova, S. P. Gromov, S. V. Dudkin, S. Yu. Zaitsev, L. Ya. Zakharova, M. A. Ziganshin, A. V. Zolotukhina, M. A. Kalinina, E. A. Karakhanov, R. R. Kashapov, O. I. Koifman, A. I. Konovalov, V. S. Korenev, A. L. Maksimov, N. Zh. Mamardashvili, G. M. Mamardashvili, A. G. Martynov, A. R. Mustafina, R. I. Nugmanov, A. S. Ovsyannikov, P. L. Padnya, A. S. Potapov, S. L. Selektor, M. N. Sokolov, S. E. Solovieva, I. I. Stoikov, P. A. Stuzhin, E. V. Suslov, E. N. Ushakov, V. P. Fedin, S. V. Fedorenko, O. A. Fedorova, Y. V. Fedorov, S. N. Chvalun, A. Yu. Tsivadze, S. N. Shtykov, D. N. Shurpik, M. A. Shcherbina and L. S. Yakimova, Functional supramolecular systems: design and applications, *Russ. Chem. Rev.*, 2021, **90**(8), 895–1107, DOI: 10.1070/RCR5011.

15 *Supramolecular Catalysis*, ed. P. W. N. M. van Leeuwen, Wiley-VCH, Weinheim, 2008.

16 D. M. Vriezema, M. Comellass Aragones, J. A. A. W. Elemans, J. J. L. M. Cornelissen, A. E. Rowan and R. J. M. Nolte, Self-Accembled Nanoreactors, *Chem. Rev.*, 2005, **105**, 1445–1490, DOI: 10.1021/cr0300688.

17 B. C. Pemberton, R. Raghunathan, S. Volla and J. Sivaguru, From Containers to Catalysts: Supramolecular Catalysis within Cucurbiturils, *Chem. – Eur. J.*, 2012, **18**, 12178–12190, DOI: 10.1002/chem.201202083.

18 S. P. Gromov and M. V. Alfimov, Supramolecular organic photochemistry of crown-ether-containing styryl dyes, *Russ. Chem. Bull.*, 1997, **46**, 611–636, DOI: 10.1007/BF02495186.

19 M. Takeshita and M. Irie, Photoresponsive Tweezers for Alkali Metal Ions. Photochromic Diarylethenes Having Two Crown Ether Moieties, *J. Org. Chem.*, 1998, **63**, 6643–6649, DOI: 10.1021/jo980290q.

20 S. Fery-Forgues and F. Al-Ali, Bis(azacrown ether) and bis(benzocrown ether) dyes: butterflies, tweezers and rods in cation binding, *J. Photochem. Photobiol. C*, 2004, **5**, 139–153, DOI: 10.1016/j.jphotochemrev.2004.07.001.

21 S. P. Gromov, Molecular meccano for light-sensitive and light-emitting nanosized systems based on unsaturated and macrocyclic compounds, *Russ. Chem. Bull.*, 2008, **57**, 1325–1350, DOI: 10.1007/s11172-008-0174-9.

22 A. I. Vedernikov, D. V. Kondratuk, N. A. Lobova, T. M. Valova, V. A. Barachevskii, M. V. Alfimov and S. P. Gromov, New cation-'capped' complex of the *Z*-isomer of a crown-containing styryl dye bearing a long *N*-ammonioalkyl substituent, *Mendeleev Commun.*, 2007, **17**, 264–267, DOI: 10.1016/j.mencom.2007.09.005.

23 Y. Liu, M. Fan, S. Zhang, X. Shenga and J. Yao, Basic amino acid induced isomerization of a spiropyran: towards visual recognition of basic amino acids in water, *New J. Chem.*, 2007, **31**, 1878–1881, DOI: 10.1039/B713247F.

24 E. N. Ushakov, M. V. Alfimov and S. P. Gromov, Design principles for optical molecular sensors and photocontrolled receptors based on crown ethers, *Russ. Chem. Rev.*, 2008, **77**(1), 39–58, DOI: 10.1070/RC2008v077n01ABEH003757.

25 M. Natali and S. Giordani, Molecular switches as photocontrollable "smart" receptors, *Chem. Soc. Rev.*, 2012, **41**, 4010–4029, DOI: 10.1039/c2cs35015g.

26 X. Xie, G. Mistlberger and E. Bakker, Reversible Photodynamic Chloride-Selective Sensor Based on Photochromic Spiropyran, *J. Am. Chem. Soc.*, 2012, **134**, 16929–16932, DOI: 10.1021/ja307037z.

27 M. Qin, Y. Huang, F. Li and Y. Song, Photochromic sensors: a versatile approach for recognition and discrimination, *J. Mater. Chem. C*, 2015, **3**, 9265–9275, DOI: 10.1039/C5TC01939G.

28 J. Sheng, S. Crespi, B. L. Feringa and S. J. Wezenberg, Supramolecular control of unidirectional rotary motion in a sterically overcrowded photoswitchable receptor, *Org. Chem. Front.*, 2020, **7**, 3874–3879, DOI: 10.1039/D0QO01154A.

29 S. J. Wezenberg, Photoswitchable molecular tweezers: isomerization to control substrate binding, and what about *vice versa*?, *Chem. Commun.*, 2022, **58**, 11045–11058, DOI: 10.1039/D2CC04329G.

30 Q. Chen, Y. Wang, J. Zhai and X. Xie, Photoswitchable hemithioindigo inspired copper ion selective sensing with excellent selectivity and versatile operational modes, *Sens. Actuators, B*, 2023, **381**, 133437, DOI: 10.1016/j.snb.2023.133437.

31 Y. Cheng, X. Ma, J. Zhaibc and X. Xie, Visible light responsive photoacids for subcellular pH and temperature correlated fluorescence sensing, *Chem. Commun.*, 2023, **59**, 1805–1808, DOI: 10.1039/D2CC06816H.

32 A. Kerckhoffs, I. Moss and M. J. Langton, Photo-switchable anion binding and catalysis with a visible light responsive halogen bonding receptor, *Chem. Commun.*, 2023, **59**, 51–54, DOI: 10.1039/D2CC05199K.

33 S. N. Dmitrieva, A. I. Vedernikov, E. N. Ushakov, L. G. Kuz'mina and S. P. Gromov, Synthesis of benzoazacrown ethers by transformation of benzocrown macrocycle and preparation of related complexing agents, *Russ. Chem. Bull.*, 2015, **64**, 1726–1745, DOI: 10.1007/s11172-015-1068-2.

34 E. N. Ushakov, A. I. Vedernikov, N. A. Lobova, S. N. Dmitrieva, L. G. Kuz'mina, A. A. Moiseeva, J. A. K. Howard, M. V. Alfimov and S. P. Gromov, Supramolecular dimerization and [2+2] photocycloaddition reactions of crown ether styryl dyes containing a tethered ammonium group: structure–property relationships, *J. Phys. Chem. A*, 2015, **119**, 13025–13037, DOI: 10.1021/acs.jpca.5b10758.

35 S. P. Gromov, S. N. Dmitrieva, A. I. Vedernikov, N. A. Kurchavov, L. G. Kuz'mina, S. K. Sazonov, Yu. A. Strelenko, M. V. Alfimov, J. A. K. Howard and E. N. Ushakov, Synthesis, structure, and characterization of chromo(fluoro)ionophores with cation-triggered emission based on N-methylaza-crown-ether styryl dyes, *J. Org. Chem.*, 2013, **78**, 9834–9847, DOI: 10.1021/jo401555a.

36 J. A. Gavin, M. E. Garcia, A. J. Benesi and T. E. Mallouk, Chiral Molecular Recognition in a Tripeptide Benzylviologen Cyclophane Host, *J. Org. Chem.*, 1998, **63**, 7663–7669, DOI: 10.1021/jo980352c.

37 W. G. Bardsley, J. S. Ashford and C. M. Hill, Synthesis and oxidation of aminoalkyl-onium compounds by pig kidney diamine oxidase, *Biochem. J.*, 1971, **122**, 557–567, DOI: 10.1042/bj1220557.

38 S. P. Gromov, O. A. Fedorova, A. I. Vedernikov, V. V. Samoshin, N. S. Zefirov and M. V. Alfimov, Synthesis of formyl derivatives of benzocrown ethers containing N, S, and O heteroatoms in the macrocycle, *Russ. Chem. Bull.*, 1995, **44**, 116–123, DOI: 10.1007/BF00696971.

39 S. P. Gromov, S. N. Dmitrieva, A. I. Vedernikov, L. G. Kuz'mina, A. V. Churakov, Y. A. Strelenko and J. A. K. Howard, Novel promising benzoazacrown ethers as a result of ring transformation of benzocrown ethers: synthesis, structure, and complexation with Ca^{2+}, *Eur. J. Org. Chem.*, 2003, 3189–3199, DOI: 10.1002/ejoc.200300179.

40 S. P. Gromov, S. N. Dmitrieva, A. I. Vedernikov, N. A. Kurchavov, L. G. Kuz'mina, Yu. A. Strelenko, M. V. Alfimov and J. A. K. Howard, *N*-Methylbenzoazacrown ethers with the nitrogen atom conjugated with the benzene ring: the improved synthesis and the reasons for the high stability of complexes with metal and ammonium cations, *J. Phys. Org. Chem.*, 2009, **22**, 823–833, DOI: 10.1002/poc.1527.

41 V. G. Avakyan, D. V. Kondratuk, A. I. Vedernikov, L. G. Kuz'mina, V. Y. Rudjak, J. A. K. Howard, M. V. Alfimov and S. P. Gromov, Formation of dimeric and cation-'capped' complexes by crown-ether styryl dyes: a DFT and X-ray study, *J. Mol. Struct.*, 2009, **935**, 136–143, DOI: 10.1016/j.molstruc.2009.07.004.

42 A. I. Vedernikov, S. N. Dmitrieva, L. G. Kuz'mina, N. A. Kurchavov, Y. A. Strelenko, J. A. K. Howard and S. P. Gromov, Benzoaza-15-crown-5 ethers: synthesis, structure, and complex formation with metal and ethylammonium ions, *Russ. Chem. Bull.*, 2009, **58**, 978–1001, DOI: 10.1007/s11172-009-0127-y.

43 V. I. Yuzhakov, Association of Dye Molecules and Its Spectroscopic Manifestation, *Russ. Chem. Rev.*, 1979, **48**(11), 1076–1091, DOI: 10.1070/RC1979v048n11ABEH002430.

44 E. N. Ushakov, S. P. Gromov, O. A. Fedorova, Yu. V. Pershina, M. V. Alfimov, F. Barigilletti, L. Flamigni and V. Balzani, Sandwich-Type Complexes of Alkaline-Earth Metal Cations with a Bisstyryl Dye Containing Two Crown Ether Units, *J. Phys. Chem. A*, 1999, **103**, 11188–11193, DOI: 10.1021/jp9929420.

45 T. P. Martyanov, E. N. Ushakov, V. A. Savelyev and L. S. Klimenko, Crown-containing naphtho- and anthraquinones: synthesis and complexation with alkali and alkaline-earth metal cations, *Russ. Chem. Bull.*, 2012, **61**, 2282–2294, DOI: 10.1007/s11172-012-0323-z.